The influence of sediment lithification on K-Ar ages and chemical zoning of glauconites

Autor(en): **Fischer, H. / Steiger, R.H.**

Objekttyp: **Article**

Zeitschrift: **Schweizerische mineralogische und petrographische Mitteilungen = Bulletin suisse de minéralogie et pétrographie**

Band (Jahr): **68 (1988)**

Heft 2

PDF erstellt am: **25.04.2024**

Persistenter Link: https://doi.org/10.5169/seals-52060

SCHWEIZ. MINERAL. PETROGR. MITT. 68, 203-214, 1988

The influence of sediment lithification on K-Ar ages and chemical zoning of glauconites

by *H. Fischer*[1] and *R.H. Steiger*[1]

Abstract

Four glauconite samples (K_2O of 6.9 to 8.5 wt%) from Switzerland were investigated by thin-section, X-ray and microprobe analysis and in particular by K-Ar dating. They were extracted from sediments which were subjected to variable degrees of lithification and which represent four different chronostratigraphic units. The results imply a correlation between extent of lithification caused by tectonization and deviation from the predicted geologic age. Thin-sections show that glauconite from strongly lithified sediments commonly contains inclusions of pyrite and apatite, whereas glauconites from unlithified sediments are free of such inclusions. Electron microprobe and element distribution scan analyses indicate firstly that the original chemical zoning of glauconite grains disappears and secondly that the replacement of glauconite by apatite increases with progressing lithification. A similar relationship is inferred from the Al–Fe–Mg-concentrations: with increasing degree of lithification glauconite is depleted in Fe and enriched in Al and/or Mg. All of these changes are believed to concur with the formation of pyrite during tectonization and to be directly correlated with the decrease in the K-Ar age.

Key words: K-Ar ages, glauconites, age deviations, sediment lithification, Helvetic Alps.

1. Introduction

Mineral phases, ranging from glauconitic smectite to glauconitic mica ("glauconite") are frequently used for the dating of sediments. However, glauconite data often provide dates that are too young, or sometimes too old, in comparison with field evidence. This observation and the reason for it has already been thoroughly discussed by many authors (e.g. EVERNDEN et al., 1960; WEBB et al., 1963; THOMPSON and HOWER, 1973; CONRAD et al., 1982; ODIN and DODSON, 1982).

HURLEY (1966) and ODIN (1982b) showed that glauconite partially recrystallizes with increasing temperature and pressure. FREY et al. (1973) investigated glauconites of Cretaceous age from the Helvetic Alps in Eastern Switzerland. They attributed the severely reduced glauconite K-Ar ages along the northern margin of the area to Alpine metamorphism and/or to tectonic overprinting. CONRAD et al. (1982) show that Alpine deformation led to isotopic rejuvenation of glauconite K-Ar ages in the Subalpine chains of Haute-Provence (SE France).

With respect to compositional variation of glauconite, a relationship between iron content and burial diagenesis was established by IRELAND et al. (1983). Based on mineralogical and chemical data, they inferred that glauconite tends to lose iron progressively during burial diagenesis. The present study examines some of the processes which occur in glauconite during lithification of sedimentary rocks and their coincidence with significant shifts in glauconite K-Ar ages.

2. Sample description

Figure 1 represents a simplified geological map of the northern part of Switzerland with its main geologic domains: 1) The Jura moun-

[1] Laboratory for Isotope Geochemistry ETH, CH-8092 Zurich, Switzerland.

tains consisting of Mesozoic sediments, folded in middle to late Miocene times, 2) the Molasse Basin filled with Oligocene and Miocene detrital sediments, mainly derived from the rising Alps; and, 3) the Helvetic belt of the Alps interpreted as northern continental shelf of the Tethys sea.

Sample locality "R" (Randen Hills, near Schaffhausen):

The Upper Jurassic (Lower Oxfordian) sample from the Randen Hills near Schaffhausen is an unlithified sediment of about 10 cm thickness that has never been stressed tectonically, the overburden did not exceed 300 m. The Oxfordian horizon is an unlithified, dark grey marl with as much as 30% glauconite together with some quartz and biotite. The bed is rich in the two ammonites *Perisphinctes (Otosphinctes) paturattensis* and *Cardioceras s. str. sp.* (GYGI and MCDOWELL, 1970, p. 113).

Sample locality "P" (Mt. Pilatus, near Lucerne):

The Eocene, Albian and Hauterivian samples from Mt. Pilatus near Lucerne are differentially lithified sediments that have been tectonized (FISCHER, 1983). Generally, no method exists to quantify the sample hardness or degree of lithification but the mesoscopic differences are easily seen. Porosity seems to approximately represent the degree of lithification. Thus, the porosity of each sample was measured with a mercury porosity meter (see Tab. 4 and Fig. 6).

The Eocene sample is weakly lithified; it is a marly calcareous sandstone with a glauconite content of about 15%. This glauconitic calcareous sandstone has a biostratigraphic age of Middle Lutetian containing numerous discocyclines and nummulites (HERB, 1983). The Albian rocks are strongly lithified. This marly sandstone, containing about 18% glauconite, is approximately 5 m thick. Ammonites indicate a Middle Albian age (FICHTER, 1934). The Upper Hauterivian to Lower Barremian layer has a constant thickness of 1.6 m. This very strongly lithified glauconite-bearing sediment is transitional between packstone and grainstone (DUNHAM, 1962) or biosparite (FOLK, (1959). At the base of this horizon occur numerous fragments of phosphorites, broken belemnites and limy rounded rock fragments. The glauconite content is highly variable

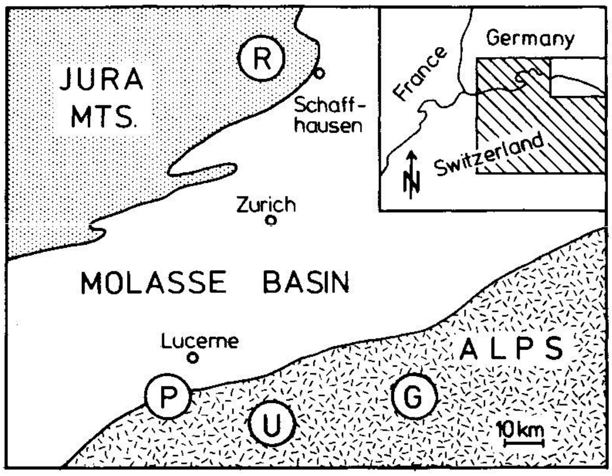

Fig. 1 Sample localities (see FISCHER, 1985, p. 222; Gygi, 1969, p. 18). Part of NE Switzerland with its three main geologic subdivisions. R: Randen hills (Jura Mts.) P: Mt. Pilatus (Helvetic nappes) U: Urnersee region G: Glarus Alps (see text, in particular discussion)

within the stratigraphic section with a mean of about 20%. The Lower Cretaceous glauconitic beds are well known key-horizons and are biostratigraphically dated by ammonites (BAUMBERGER et al., 1907).

3. Mineral separation

Glauconite pellets of grain size 160 to 500 μm were purified by washing, crushing (when needed), magnetic separation and hand picking. No acids were used during the separation procedure. To reduce the effects of inhomogeneity about ten times the required quantity was handpicked and all samples were split using a microsplitter.

4. Thin section observations and interpretation

4.1. INCLUSIONS

Under the microscope glauconite grains from the Oxfordian and Eocene samples are homogeneous and contain no inclusions except for occasional grains of opaques. Thinsections from the strongly lithified Albian and Hauterivian samples, in contrast, show numerous inclusions of euhedral pyrite, dolomite and calcite in the glauconite grains (Fig. 2 and 4). Apart from these inclusions, the glauconite grains appear to be optically very homogene-

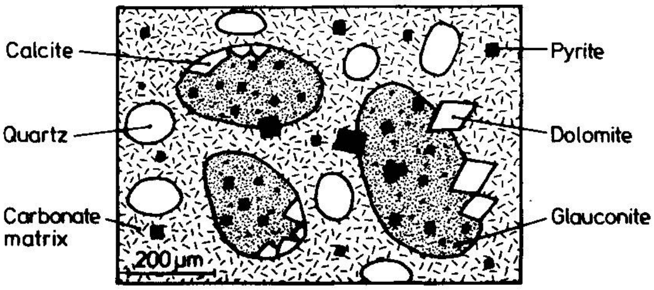

Fig. 2 Microscope observation in thin-section of a strongly lithified sample (e.g. Hauterivian).

ous. The calcite and dolomite crystals occur mostly at grain boundaries, whereas pyrite is included within the glauconite grains and in the carbonate matrix. The dolomite crystals are generally idiomorphic and - in contrast to the calcite crystals growing on the inside - have overgrown the pre-existing boundary of the glauconite grain (Fig. 2).

4.2. PRESSURE SHADOWS

Within a single glauconite horizon of the Altmannschichten, located at Klimsen (Mt. Pilatus), variation in the influence of tectonization may be seen between the different lithologies. In the sandy clay, well developed calcite pressure shadows were detected around glauconite grains (Fig. 3). Such grains are mineralogically very homogeneous, containing practically no inclusions. These pressure shadows occur only in the top layer of the consolidated 7 m thick glauconitic horizon (Fig. 4). Presumably, the pressure shadows formed because

1. the grain dimensions of the clayey carbonate matrix and the glauconite crystals differ by orders of magnitude,
2. this layer was very weakly cemented as compared to the calcareous, glauconite rich horizon below.

The pressure shadows comprise aggregates of new calcite grains growing on opposite sides of the glauconite grains, thereby producing an elongate structure ("lineation"). The direction of these pressure shadows is exactly parallel with the prevailing stress field during nappe emplacement in the Pilatus region (Fischer, 1983). It seems, that this clayey layer must have borne the major impact of deformation. For lack of sufficient material it was not possible to perform an age determination on such tectonically stressed glauconite pellets.

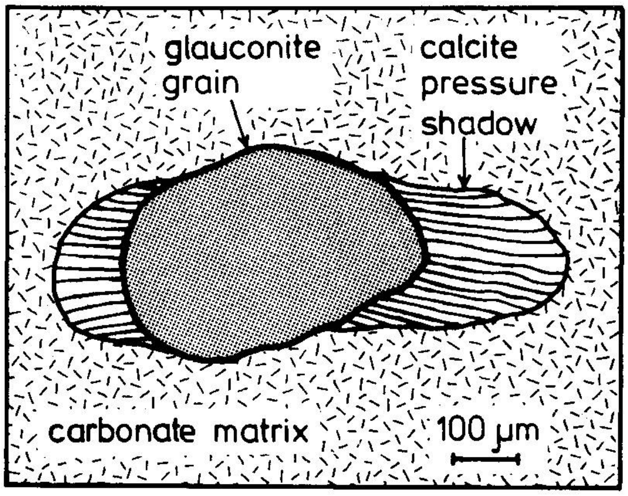

Fig. 3 Pressure shadows of calcite on a single glauconite grain. Detailed investigation showed that the growth direction was antitaxial.

Immediately below the top layer (Fig. 4) with pressure shadows, the glauconite is of the type shown in Fig. 2. In the inverted lower and strongly thinned limb of the fold (Fig. 4), the glauconite grains are usually mantled by calcite crystals (Fig. 5). Occasionally, only small relics of glauconite are left (Figs. 4 and 5).

5. Electron microprobe analyses

5.1. ZONED STRUCTURE

In their original study, Valeton and Abdul-Razzak (1974) distinguished between dark, chemically homogeneous and pale chemically heterogeneous glauconite grains. In addition, the dark pellets were significantly enriched in potassium as well as in SiO_2. Velde and Odin (1975) explained the existence of an aluminium-rich and iron-poor external zone in glauconite pellets as a gradient in the chemical activity of these elements. The chemical changes taking place during the formation of glauconite were investigated at four different stages of development by Birch et al. (1976). Cook and Marshall (1981) studied iron and phosphorus-rich glauconitic nodules from the East Australian continental shelf by electron microprobe. They found a geochemical similarity with glauconite pellets from the continental margin of northern Spain. The high concentration of phosphate in the interstitial water, which lead to precipitation of apatite, is explained as a result of mass mortality of ammonites and belemnites.

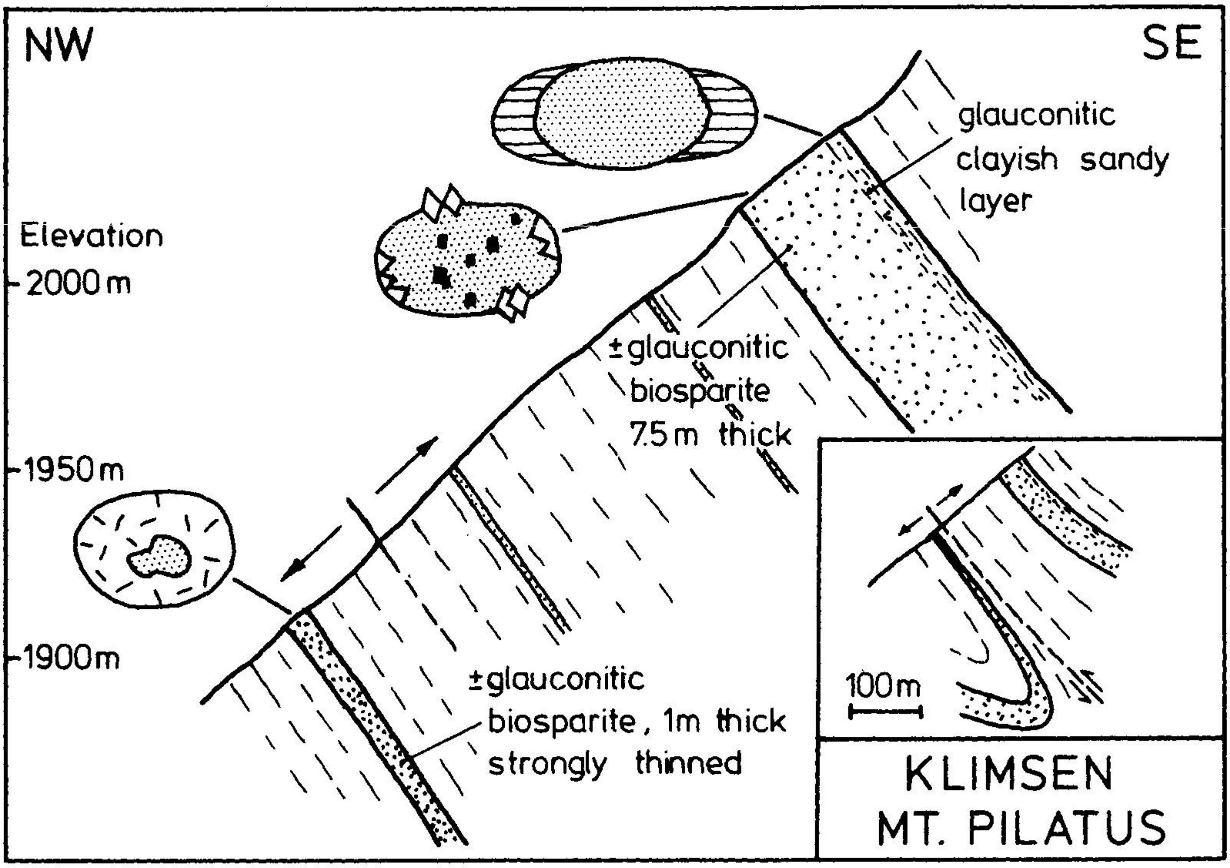

Fig. 4 Schematic sketch profile of the tectonized glauconitic «Altmann»-strata (Hauterivian / Barremian) at Mt. Pilatus. The upper part is the normal limb in its original thickness, whereas the overturned limb, below, was strongly thinned tectonically (thickness not to scale). The arrows indicate the normal stratigraphic sequence. One can distinguish three kinds of glauconite grains:

1. glauconite grains with calcite pressure shadows in a clayish sandy layer at the top of the upper limb (Fig. 3)
2. glauconite grains with various inclusions in a lithified biosparite (Fig. 2)
3. glauconite grains extensively replaced by calcite and occurring only in the strongly thinned overturned limb (Fig. 5).

For the present study glauconite grains from all four samples were analyzed by electron microprobe. Grains with diameters of about 500 μm were selected. A profile of ten points was measured along and perpendicular to the longest grain diameter. The profiles are arranged from top to bottom in Fig. 6 in order of increasing degree of lithification (= decreasing porosity). For the sake of clearness, only one of the two perpendicular profiles was drawn. The asymmetrical curves result from grains whose polished surfaces were off-center.

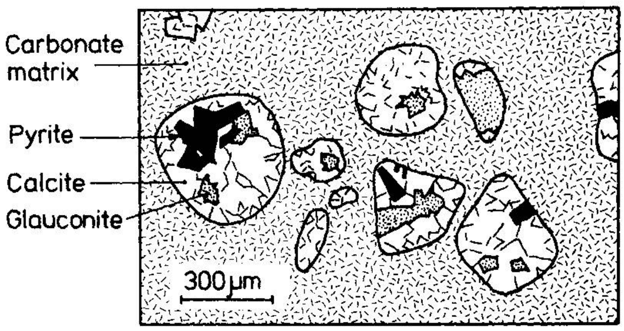

Fig. 5 Recrystallized glauconite grains which have been partially transformed into calcite crystals. This kind of grains occurs in zones of intensive tectonical strain.

The following observations can be made:

- for both grain traverses the results are similar,
- glauconite grains from loose or weakly lithified sediments show distinct chemical zonation,
- the Al-content in such grains shows a minimum at the center and increases towards the margins,
- for total iron we see a reverse trend: in uncompacted sediments the maximum content is in the grain center whereas the minimum is at the grain boundary,

- this pattern becomes blurred with increasing degree of lithification.

This suggests that lithification of the rock leads to homogenization of the glauconite grains. Oddly enough, the potassium content and distribution does not vary with the degree of rock lithification. The total Fe-content exhibits no distinct correlation with the K-content, in accordance with the results of IRELAND et al. (1983) and DE GRAVE et al. (1985).

5.2. GLAUCONITE-APATITE INTERGROWTH

Many inclusions could not be identified by microscopic techniques. However, element distribution scans show similar distributions for P and Ca in the grains (Fig. 7). X-ray diffraction analyses confirm the presence of glauconite-apatite-intergrowths and/or exsolution of apatite group minerals in glauconite from the tectonically stressed Hauterivian sample (Fig. 8). Furthermore, the peak at $2\Theta = 13°$ in the diffractogramm of this sample points to diagenetic growth of a Fe-rich chlorite. In contrast, glauconite grains from uncompacted sediments do not show this feature. Therefore it appears that the occurrence of apatite in glauconite is related to the process of lithification caused by tectonization. In contrast, HALDIMANN (1977, p. 150) rather assumed an inorganic origin from colloidal apatite (collophane).

5.3. CHEMICAL VARIATION OF GLAUCONITES AND THE FORMATION OF PYRITE

The chemical changes taking place in glauconite during lithification of the rock are illustrated in Tab. 1: Iron becomes depleted with increasing degree of lithification, whereas aluminium and magnesium are enriched. These chemical trends are presented in an Al-Fe-Mg diagram (Fig. 9). The data from all four samples show a well-defined correlation between degree of lithification and chemical composition: with increasing lithification iron is concentrated in the form of pyrite, either within the grain itself or in the surrounding matrix. This trend is visible by mesoscopic inspection of the rock specimen.

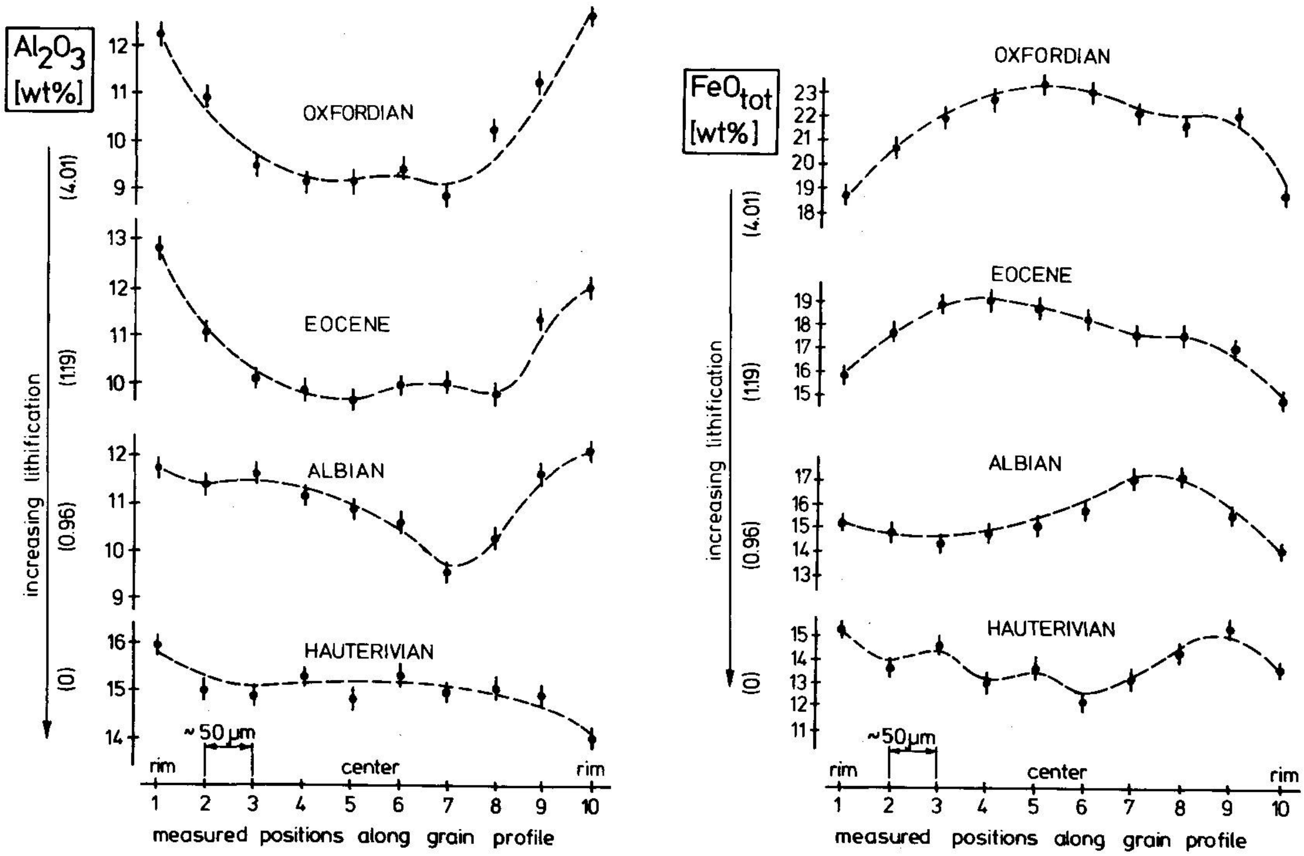

Fig. 6 Influence of lithification on Al_2O_3 and FeO_{tot} concentration. Numbers in parentheses represent the porosity in equivalent surface [m^2/g sample].

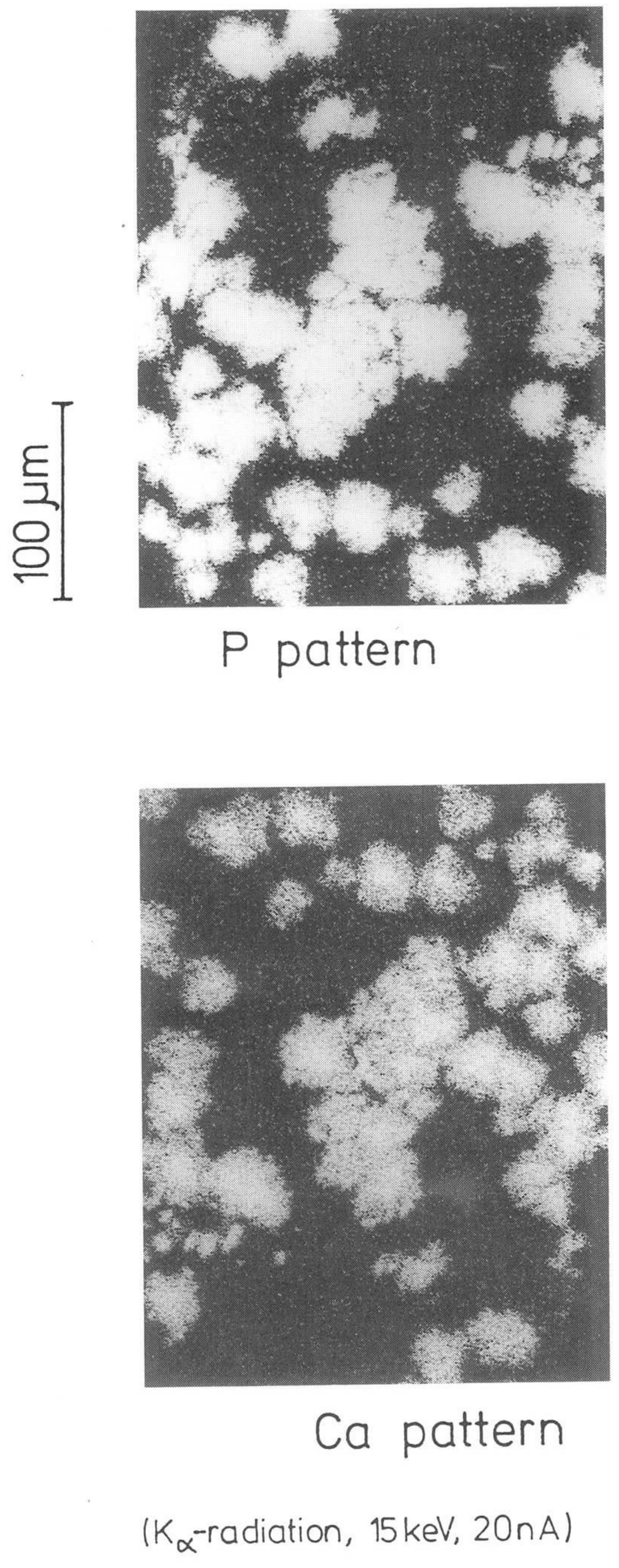

Fig. 7 Pattern of phosphorus and calcium distribution in a single glauconite grain from the tectonically stressed horizon (Hauterivian).
The two elements P and Ca show the same pattern. Obviously, we are looking at intergrowths of apatite group minerals.

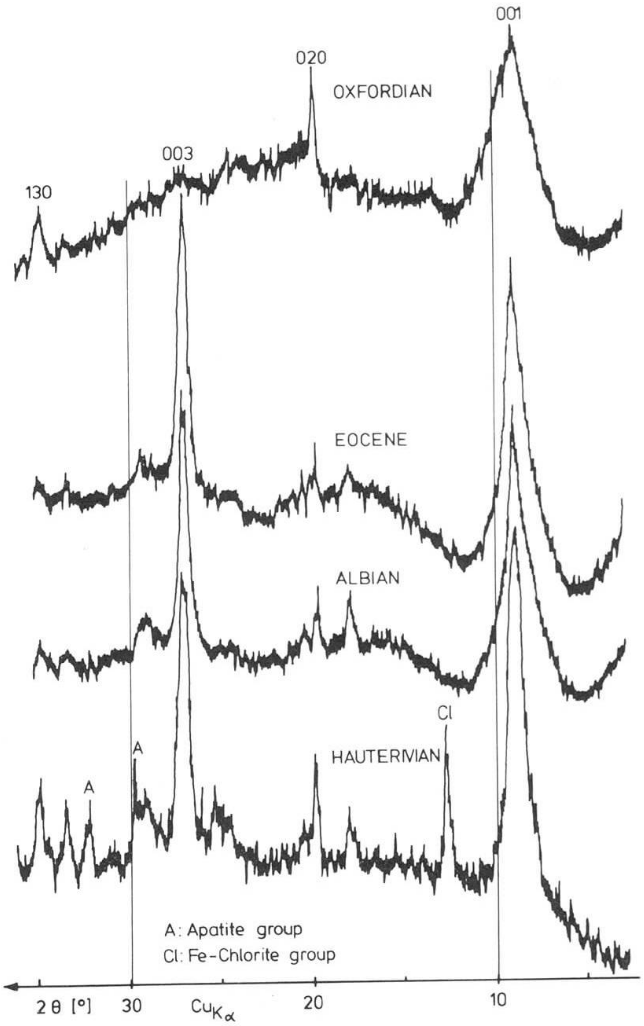

Fig. 8 X-ray diffractograms of the four investigated samples. The K-poor Oxfordian sample has a 003-peak of minor intensity; nevertheless, the K-Ar ages agree very well with biostratigraphy. Glauconite from the very strongly lithified Hauterivian sediment shows peaks for apatite and Fe-chlorite group minerals. Glauconite K-Ar ages from this horizon differ strongly from the biostratigraphic age.

This explanation is commonly accepted (McRae, 1972; Curtis and Spears, 1973; Weaver and Pollard, 1973) and supported by thermodynamic calculations which favor a diagenetic origin for the formation of pyrite. Birch et al. (1976) in tracing the chemistry of the process of glauconite formation postulate a gradual substitution of Fe for Al in the octahedral position during the formation of glauconite.

Based on our observations it must be assumed that during diagenesis overprinted by a tectonic event the reverse reaction from that observed during glauconite formation is taking place, namely substitution of Al for Fe. The

Tab. 1 Increasing lithification causes chemical changes in glauconite. The change seems to occur independently of the potassium content.

	Oxfordian	Eocene	Albian	U.Hauterivian
FeO_{tot}	22	19	16	14
Al_2O_3	9	10	11	15
MgO	2.9	4.0	4.9	5.2

——increasing lithification——→

An approximative parameter of lithification is porosity (comment see Fig. 6 and Table 4). Values in weight%.

same antithetic relationship between ferric iron and aluminium was also confirmed by IRELAND et al. (1983).

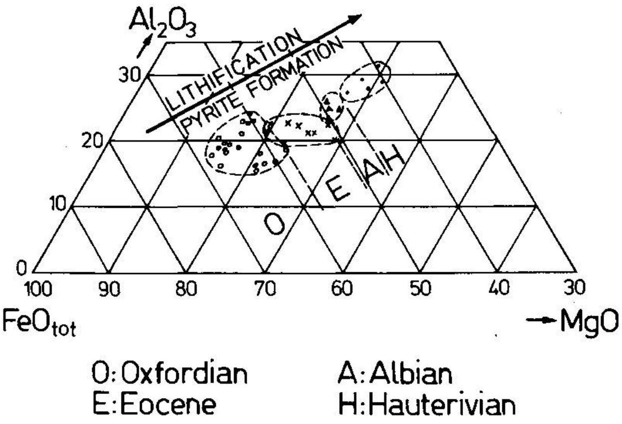

Fig. 9 Al_2O_3, FeO_{tot} and MgO representing – besides K_2O – the three dominant oxides of glauconite. Values are in mole-%, total iron as FeO. Each point in the diagram corresponds to a single electron microprobe analysis.

6. K-Ar age determinations, standard measurements

6.1. WEIGHING

Glauconite pellets are very hygroscopic. A 20% change in humidity results in a weight difference of about 1% (FISCHER, 1983). Therefore, the sample weights were taken either at constant humidity or an empirical calibration curve was used. All weights were reduced to 60% relative humidity; furthermore, sample aliquots for K and Ar determinations were weighed in close sequence.

6.2. ANALYTICAL METHODS

For several samples the K-content was measured using both isotope dilution and atomic absorption technique. The results of the two methods agree within a relative deviation of 0.6%.

The argon analyses were carried out in an all-metal rare-gas sytem of Signer-Baur design using the peak height method (DEUTSCH, 1983), i.e., without addition of ^{38}Ar spike. All samples were preheated in vacuum at a temperature of 120 °C for six hours. Ar was purified using Ag, ZrTi and ZrAl getters and was isotopically analyzed on a 12 cm, 90° mass spectrometer operated in a static mode on-line with a computer.

6.3. GLAUCONITE STANDARD GL-O

The international glauconite standard GL-O served as reference material. Potassium was analyzed by isotope dilution. Three independent measurements yielded an average K-concentration of 6.64 ± 0.03 weight%. This agrees within limits of error with the recommended value of 6.56 ± 0.06 weight% (ODIN et al., 1982). Argon concentrations are shown in Tab. 2. The seven analyses resulted in a mean radiogenic argon concentration of (2420 ± 24) $\cdot 10^{-8} cm^3/g$ STP (standard error 1σ confidence limit). The large variations up to 3% between individual sample splits of the GL-O standard point to significant sample inhomogeneity which was also confirmed for the major elements by numerous single grain measurements with the electron microprobe (FISCHER, 1983). In comparison with the mean value of (2485 ± 24) $\cdot 10^{-8} cm^3/g$ STP reported by ODIN et al. (1982) our mean Ar-concentration is low by 2.6%. Our calculated mean age corresponds to 91.5 ± 1.8 Ma (error = 95% confidence limit) and is low by 3.7% in comparison with the mean of 95.03 ± 1.11 Ma (ODIN et al., 1982). Several possible sources of error were thoroughly examined. Calibrations by standard gas (highly purified air argon) were repeatedly performed but no plausible explanation for the difference has yet been found.

6.4. K-Ar RESULTS (Tab. 3 and 4)

The data (2σ errors) for Eocene, Albian and Hauterivian samples are taken from FISCHER (1985) and are summarized in Tab. 4. The Lower Oxfordian samples (Tab. 3) originate from three neighbouring localities (GYGI,

Tab. 2 Results of the K-Ar measurements of standard GL-O.

Sample	K *)	^{36}Ar	^{40}Ar	^{40}Ar	rad. ^{40}Ar	Weight	Calc. Age
	[wt.%]	[10^{-8} cm^3/g]		[%rad]	[10^{-8} cm^3/g]	[mg] ")	[Ma] +)
1	6.64	.620	2616	93	2433+-14	13.5	92.0+-1.2
2	6.62	.579	2592	93	2421+-14	63.9	91.5+-1.2
3	6.67	.615	2592	93	2410+-14	87.8	91.1+-1.2
4		.352	2481	96	2377+-13	83.8	89.9+-1.0
5		.407	2554	95	2434+-13	43.1	92.0+-1.2
6		.344	2511	96	2410+-13	79.5	91.1+-1.2
7		.361	2560	96	2454+-13	20.9	92.7+-1.2

*) Three independent isotope dilution analyses
") Sample weights used for argon analyses
+) All seven ages were calculated with the mean K value of 6.64+-0.03%; age errors shown correspond to 2σ

1969, p. 18). Samples RG212A and RG212Gy represent two separate specimens from the same outcrop. The ages agree very well with the K-Ar age of 145 ± 3 Ma given by GYGI and MCDOWELL (1970). In Tab. 4 the glauconite K-Ar ages of the four measured samples are compared with the numerical geologic time scale (ODIN, 1982a). All ages are based on constants recommended by the IUGS-subcommission on geochronology (STEIGER and JÄGER, 1977). The error of the K-Ar model ages (2σ) is calculated by Gaussian error propagation considering the following analytical steps: weight error, regression analysis of the argon measurement to the timepoint of the gas inlet, reproducibility of the argon inter-sample and inter-run calibrations and finally the analytical error of the K-determination. Because of the generally considerable age deviations, the measured K-Ar ages were not corrected with the standard GL-O. The samples from Lower Oxfordian agree with the time scale within measurement precision, whereas the Upper Eocene (Middle Lutetian), the Albian and Hauterivian samples show ages that are much younger than expected from their stratigraphic positions (FISCHER et al., 1984). Compared with the geological time scale of HARLAND et al. (1982) the tectonized glauconites have ages even more rejuvenated and the apparently "correct" ages of the Lower Oxfordian samples would be up to 8% too young.

Furthermore, in Tab. 4, the four sample groups are arranged in order of increasing lithification. For three groups, the K_2O-content is above 7%, the lower limit for evolved to highly

Tab. 3 Results of the K-Ar measurements of the Jurassic (lower Oxfordian) glauconites. Duplicate potassium analyses by atomic absorption agree to within 1%.
Grain sizes: RG212A: 300–500 μm; RG212Gy: 200–500 μm; RG207B and RG81B: 160–300 μm.

Sample	K	^{36}Ar	^{40}Ar	^{40}Ar	rad. ^{40}Ar	Weight	Calc. Age
	[wt.%]	[10^{-8} cm^3/g]		[%rad]	[10^{-8} cm^3/g]	[mg] *)	[Ma] ")
RG212A	5.82	.879	3745	93	3486+-20	11.3	148.0+-1.8
RG212Gy	5.82	1.194	3820	91	3468+-20	7.5	147.2+-2.0
RG207B	5.67	8.290	5850	58	3401+-39	9.6	148.2+-3.4
RG81B	5.76	.515	3529	96	3377+-19	19.5	145.0+-2.4

*) Sample weights used for argon analyses
") Confidence limit: 2σ

Tab. 4 K-Ar ages in comparison with the geologic time scale and influence of lithification. The indicated degree of lithification is of qualitative nature only; the porosity should represent a measure for lithification. For analytical data of the Eocene, Albian and Hauterivian samples, see FISCHER (1985).

	Lower Oxfordian	Eocene (M.Lutetian)	Middle Albian	U.Hauter./ L.Barrem.
Geol. age [Ma] *)	145 - 150	39 - 45	95 - 107	112 - 115
Ages [Ma]	148.0+-1.8 147.2+-2.0 148.2+-3.4 145.0+-2.4	35.7+-0.8 35.6+-0.8	81.0+-1.8 80.8+-1.8	70.7+-1.8
K_2O-Content [wt.%]	6.9	8.5	8.5	7.4
Age-Reduction [%]	0 to 4	approx. 18	approx. 20	approx. 35
Degree of Lithification	unlithified	weak	strong	very strong
Porosity [m^2/g] ")	4.1	1.19	0.96	0

*) Geologic time scale after Odin (1982a)
") To quantify the degree of lithification porosity was measured with a mercury porosity meter; units in equivalent surface [m^2/g sample]

evolved ("mature") glauconites (ODIN and MATTER, 1981), whereas that for the Oxfordian samples is slightly lower.

7. Discussion

The K-Ar age reductions occur with the degree of lithification and are presumably correlated with it. Unlithified sediments show no or only minor age reduction, whereas strongly lithified rocks show a large decrease in age.

Similar conclusions were made by GRANT et al. (1984). Paleozoic glauconite pellets from Ohio and Indiana gave identical K-Ar and Rb-Sr ages which were substantially younger than the stratigraphic age of the formation. Because the burial depths of these glauconite-bearing rocks were less than 1 km, thermal resetting of the Rb-Sr and K-Ar systems was considered unlikely. The authors believe that the identical Rb-Sr and K-Ar ages refer to a specific stage in the diagenetic history of the formation. Furthermore, they suggest that this diagenetic event should have caused substantial chemical change in the glauconite leading to loss of previously accumulated ^{40}Ar.

References to environmental control on glauconite composition are contradictory (BORCHERT and BRAUN, 1963; BJERKLI and ÖSTMO-SAETER, 1973). Whole-rock X-ray fluorescence analyses show that the variation of the major oxides within the glauconite-bearing section of the Hauterivian layer at Mt. Pilatus (Fig. 4) is larger than between the investigated horizons from the different sampling localities (FISCHER, 1983). It may therefore be assumed that there was little if any environmental influence on the composition of glauconite and on its predisposition to K-Ar age reduction.

The lithified glauconite-bearing lower Cretaceous sediments of Mt. Pilatus are transitional between packstone and grainstone or biosparite. Even in homogeneous rocks there is no single criterion by which diagenetic processes can be distinguished from those of lowest grade metamorphism. According to FREY (1986, plate 1) the Pilatus area clearly lies outside of the anchizone of Alpine metamorphism. As inferred from illite "crystallinity" data (ISCHI, 1973), it corresponds to the zone of diagenesis which would roughly correlate with the zeolite facies. Tectonic units similar to the Pilatus area have been studied by BREITSCHMID

(1982) in a cross section through the external Alps, some 25 km to the SE of the Pilatus region. On the basis of illite crystallinity measurements he showed diagenesis and very low-grade metamorphism to increase from north to south. He placed the geological equivalent of the Pilatus region (See "U" in Fig. 1) within the zone of diagenesis and postulated that the boundary between diagenesis and anchimetamorphism be placed some 10 km further to the south of this location. The study by FREY et al. (1973: localities [4] and [9] in Tab. 8 and Fig. 1) lists three substantially lowered glauconite K-Ar ages from the Altmannschichten, in what these authors call "original, unmetamorphosed" Cretaceous sediments at the N margin of the Helvetic nappes N of Glarus (see "G" in Fig. 1). From later papers (FREY et al., 1980 and FREY, 1986) we glean that the sampling locality [4] for two of the above glauconites is very close to the anchizone of Alpine metamorphism to which minimum conditions of 200 °C and 1200 bar are assigned. Furthermore these latter authors conclude that postmetamorphic thrusting seems to be a common feature in the external part of the Alps. This implies that the present-day position of a Helvetic rock unit, such as the Mt. Pilatus area, may not a priori be used to infer its grade of metamorphic imprint.

As shown previously, the Pilatus rocks were clearly affected by tectonic overprint. While it is difficult to single out the major factor (diagenesis, very low-grade metamorphism, tectonic stress or overburden) leading to the lithification of glauconite bearing rocks in the Pilatus region, recrystallization of glauconites is well demonstrated by K-Ar results and the disappearence of their zoned chemical structure. Our observations support the conclusions by ODIN (1982b) that rejuvenation is not only a diffusion process but may be related to recrystallization processes. In the presence of organic chemical residues this may in turn have led to formation of the observed pyrite and glauconite-apatite intergrowths.

8. Conclusions

This study demonstrates the advantage of using a multi-method approach for the investigation of glauconite. On the basis of the experimental results, the following conslusions can be drawn:

- for uncompacted sediments practically no difference is seen between glauconite K-Ar ages and stratigraphic age
- severe age reduction, however, is seen for weakly and strongly lithified samples
- the original chemical zoning of glauconite grains disappears with increasing lithification of the sediment, caused by tectonization
- glauconites from lithified sediments contain flaky apatite crystals
- with increasing lithification iron is removed from glauconite to form pyrite in the grain itself or in the surrounding matrix
- the chemical composition of the glauconite grains is affected by lithification.

Acknowledgments

We are much obliged to P. Signer and his group for the use and maintenance of the argon mass spectrometer. Especially, we are grateful to H. Baur for assistance and advice with the gas measuring procedures and data reduction. Electron microprobe analyses were performed by P. Ulmer and G. Kahr advised on porosity determination. R. Gygi provided the Jurassic glauconite samples. We also thank F. Oberli, M. Wiedenbeck and J.-P. Benkert for critical reading of the manuscript. Reviews on an earlier version of the manuscript by V. Berg-Madsen and P.M. Holm as well as an anonymous reviewer are acknowledged. We much appreciate the helpful comments by M. Frey and H. Funk. The first author was partially supported by funds from Swiss National Science foundation Grants 2.087-0.83 and 2.401-0.84.

References

BAUMBERGER, E., HEIM, ARN. and BUXTORF, A. (1907): Paläontologisch-stratigraphische Untersuchungen zweier Fossilhorizonte an der Valanginien-Hauterivien-Grenze am Churfirsten-Mattstockgebiet. Mit einigen Bemerkungen über die Stratigraphie der analogen Schichten der Zentralschweiz. Abh. schweiz. paläont. Ges. 34, 1-33.

BIRCH, G.F., WILLIS, J.P. and RICKARD, R.S. (1976): An Electron Microprobe Study of Glauconites from the Continental Margin of the West Coast of South Africa. Marine Geol. 22, 271-283.

BJERKLI, K. and ÖSTMO-SAETER, J.S. (1973): Formation of Glauconite in Foraminiferal Shells on the Continental Shelf off Norway. Marine Geol. 14, 169-178.

BORCHERT, H. and BRAUN, H. (1963): Zum Chemismus von drei Glaukonittypen. Chemie d. Erde, 23, 82-90.

BREITSCHMID, A. (1982): Diagenese und schwache Metamorphose in den sedimentären Abfolgen der Zentralschweizer Alpen (Vierwaldstätter See, Urirotstock). Eclogae geol. Helv. 75/2, 331-380.

CONRAD, M., KREUZER, H. and ODIN, G.S. (1982): Potassium-argon dating of tectonized glauconites. In: Numerical Dating in Stratigraphy (Ed. by G.S. Odin), pp. 321-332. Wiley, Chichester.

COOK, P.J. and MARSHALL, J.F. (1981): Geochemistry of Iron and Phosphorus-rich Nodules from the East Australian Continental Shelf. Marine Geol. 41, 205-221.

CURTIS, C.D. and SPEARS, D.A. (1968): The Formation of Sedimentary Iron Minerals. Econ. Geol. 63, 257-270.

DE GRAVE, E., VANDENBRUWAENE, J. and ELEWAUT, E. (1985): An ^{57}Fe Mössbauer Effect Study on Glauconites from different locations in Belgium and Northern France. Clay Miner. 20, 171-179.

DEUTSCH, A. (1983): Datierungen an Alkaliamphibolen und Stilpnomelan aus der südlichen Platta-Decke (Graubünden). Eclogae geol. Helv. 76/2, 295-308.

DUNHAM, R.J. (1962): Classification of carbonate rocks according to depositional texture. In: Classification of carbonate rocks. Amer. Assoc. Petrol. Geol. Mem. 1, 108-121.

EVERNDEN, J.F., CURTIS, G.H., KISTLER, R.W. and OBRADOVICH, J. (1960): Argon Diffusion in Glauconite, Microcline, Sanidine, Leucite and Phlogopite. Amer. J. Sci. 258, 583-604.

FICHTER, H.J. (1934): Geologie der Bauen-Brisen-Kette am Vierwaldstättersee und die zyklische Gliederung der Kreide und des Malm der helvetischen Decken. Beitr. geol. Karte Schweiz, N.F., 69. Liefg., 128 p.

FISCHER, H. (1983): K-Ar und Rb-Sr-Altersbestimmungen an Glaukoniten der Helvetischen Kreide, des Tertiärs und des Oberen Jura sowie Geologie des Nord-Pilatus. Unpubl. Diploma Thesis, University of Zurich, 215 p.

FISCHER, H. (1985): Grenzen der K-Ar-Datierung an Glaukoniten im Pilatusgebiet (Helvetikum). Eclogae geol. Helv. 78/2, 221-233.

FISCHER, H., BAUR, H. and STEIGER, R.H. (1984): The Influence of Cementation on Glauconite K-Ar Ages and Pyrite Formation. Abstract. Terra cognita 4, 204.

FOLK, R.L. (1959): Practical petrographic classification of limestones. Bull. Amer. Assoc. Petrol. Geol. 43, 1-38.

FREY, M. (1986): Very low-grade metamorphism of the Alps - an introduction. Schweiz. mineral. petrogr. Mitt. 66, 13-27.

FREY, M., TEICHMÜLLER, M., TEICHMÜLLER, R., MULLIS, J., KÜNZI, B., BREITSCHMID, A., GRUNER, U. and SCHWIZER, B. (1980): Very low-grade metamorphism in external parts of the Central Alps: Illite crystallinity, coal rank and fluid inclusion data. Eclogae geol. Helv. 73/1, 173-203.

FREY, M., HUNZIKER, J.C., ROGGWILLER, P. and SCHINDLER, C. (1973): Progressive niedriggradige Metamorphose glaukonitführender Horizonte in den helvetischen Alpen der Ostschweiz. Contr. Mineral. Petrol. 39, 185-218.

GRANT, N.K., LASKOWSKI, T.E. and FOLAND, K.A. (1984): Rb-Sr and K-Ar Ages of Paleozoic Glauconites from Ohio-Indiana and Missouri, U.S.A. Isot. Geosci. 2, 217-239.

GYGI, R.A. (1969): Zur Stratigraphie der Oxford-Stufe (oberes Jura-System) der Nordschweiz und des süddeutschen Grenzgebietes. Beitr. geol. Karte Schweiz, N.F., 136. Liefg., 123 p.

GYGI, R.A. and MCDOWELL, F.W. (1970): Potassium-Argon Ages of Glauconites from a biochronologically dated Upper Jurassic sequence of Northern Switzerland. Eclogae geol. Helv. 43, 85-97.

HALDIMANN, P.A. (1977): Sedimentologische Entwicklung der Schichten an einer Zyklengrenze der Helvetischen Unterkreide: Pygurus-Schichten und Gemsmättli-Schicht (Valanginian/Hauterivian) zwischen Thunersee und St. Galler Rheintal. Diss. ETH Zürich, Nr. 6061, 184 p.

HARLAND, W.B., COX, A.V., LLEWELLYN, P.G., PICKTON, C.A.G., SMITH, A.G. and WALTERS, R. (1982): A Geologic Time Scale. Cambridge Univ. Press, Cambridge, 131 p.

HERB, R. (1983): Eozän von Foribach bei Sarnen: In BAYER et al.: Bericht über die Jubiläumsexkursion «Der Faziesbegriff und die Sedimentationsprozesse» der Schweizerischen Geologischen Gesellschaft vom 12. bis 17. September 1982 (p. 149-157). Eclogae geol. Helv. 76/1, 125-180.

HURLEY, P.M. (1966): K-Ar Dating of Sediments. In: Potassium Argon Dating (Ed. by Schaeffer & Zähringer), pp. 134-151. Springer, Berlin.

IRELAND, B.J., CURTIS, C.D. and WHITEMAN, J.A. (1983): Compositional variation within some glauconites and illites and implications for their stability and origins. Sedimentology 30, 769-786.

ISCHI, H. (1973): Geologie des Risetenstock-Gebietes in der Schafmatt-Schimbrig-Kette (Entlebuch, LU). Unpubl. Diploma Thesis, University of Berne, 81 p.

MCRAE, S.G. (1972): Glauconite. Earth-Sci. Rev. 8, 397-440.

ODIN, G.S. (1982a): The Phanerozoic Time Scale revisited. Episodes 3, 3-9.

ODIN, G.S. (1982b): Effect of pressure and temperature on clay mineral potassium-argon ages. In: Numerical Dating in Stratigraphy (Ed. by G.S. Odin), pp. 307-319. Wiley, Chichester.

ODIN, G.S. and DODSON, M.H. (1982): Zero isotopic age of glauconites. In: Numerical Dating in Stratigraphy (Ed. by G.S. Odin), pp. 277-305. Wiley, Chichester.

ODIN, G.S. and MATTER, A. (1981): De glauconiarum origine. Sedimentology 28, 611-641.

ODIN, G.S. and 35 COLLABORATORS (1982): Interlaboratory standards for dating purposes. In: Numerical Dating in Stratigraphy (Ed. by G.S. Odin), pp. 123-150. Wiley, Chichester.

STEIGER, R.H. and JÄGER, E. (1977): Subcommission on geochronology: Convention on the use of decay constants in geo- and cosmochronology. Earth and planet. Sci. Lett. 36, 359-362.

THOMPSON, G.R. and HOWER, J. (1973): An explanation for low radiometric ages from glauconite. Geochim. cosmochim. Acta 37, 1473-1491.

VALETON, I. and ABDUL-RAZZAK, A. (1974): Der Glaukonit aus dem Essener Grünsand (Cenoman-Krc$_{2-3}$) in Essen. Mitt. geol.-paläont. Inst. Univ. Hamb. 43, 85-97.

VELDE, B. and ODIN, G.S. (1975): Further information related to the origin of glauconites. Clays and Clay Miner. 23, 376–381.

WEAVER, C.E. and POLLARD, L.D. (1973): The Chemistry of Clay minerals. Elsevier, Amsterdam, 213 p.

WEBB, A.W., MCDOUGALL, I. and COOPER, J.A. (1963): Retention of Radiogenic argon in Glauconites from Proterozoic Sediments, Northern Territory, Australia. Nature 199, 270-271.

Manuscript received June 9, 1988; revised manuscript accepted July 14, 1988